

# A new magnetic resonance imaging probe specifically targeting vascular endothelial growth factor receptor 2: synthesis, characterization and biological evaluation

Xiaoguang You<sup>1,2</sup> and Yikai Xu<sup>1,\*</sup>

<sup>1</sup>Department of Radiology, The Affiliated Hospital of Southern Medical University, Nanfang Hospital, No. 1838, Guangzhou Ave, Guangzhou, China 510000

<sup>2</sup>Department of Radiology, The Affiliated Hospital of Hainan Medical University, No. 31, Longhua Road, Haikou, China 571100

**Vascular endothelial growth factor (VEGF) is strongly expressed in most tumours and promotes both tumour growth and vascularization. The peptide, VEGF<sub>125-136</sub>, consisting of 12 amino acids is encoded by exon 6 of the VEGF gene and inhibits VEGF activity by blocking the binding of VEGF to the VEGFR2 receptor. The aim of the present study was to develop a targeting probe for magnetic resonance imaging (MRI) of tumours by conjugating VEGF<sub>125-136</sub> to gadolinium (III) (Gd(III)) (VGd) through the formation of chelates. The targeting efficiency of VGd to human hepatocellular carcinoma (HCC) cell line, BEL-7402, was subsequently determined both *in vitro* and *in vivo*. In the *in vitro* studies, the MRI results of BEL-7402 cells treated with VGd showed significantly higher T1 signal-to-noise ratio than that of both the competitive group, namely, those treated with VGd and VEGF<sub>125-136</sub> and the control group, a scramble peptide conjugated to Gd(III) (SGd). *In vivo*, when xenografts of BEL-7402 cells were established in mice and then VGd or SGd were injected via tail vein, MRI showed that the tumour signal from VGd initially decreased from 5 to 120 min and then it increased at 120 min post injection. The peak signal was observed at 120 min after injection. In contrast, no distinct peak was observed for SGd. These findings indicate that VGd can target VEGFR2, highly expressed by BEL-7402 cells, enabling targeting MRI with high efficacy to be achieved both *in vitro* and *in vivo*.**

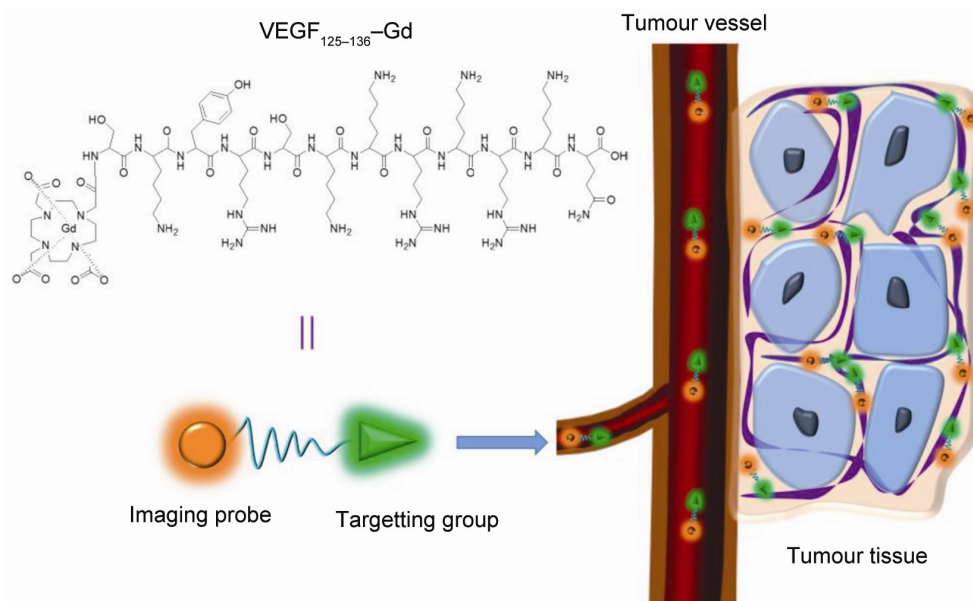
**Keywords:** Gadolinium, liver cancer xenograft, MRI, peptide, VEGF<sub>125-136</sub>.

CANCER is one of the most serious diseases that threaten human beings, and an early diagnosis of tumours, particularly small ones, is of great importance for improving patient prognosis. Thus, an important task for molecular imaging is to generate accurate images that can facilitate

early diagnosis of cancers<sup>1</sup>. Most of the tumour-imaging agents currently used for MRI in clinics are gadolinium (Gd) or iron-based contrast agents, which generally image soft tissues with high spatial resolution and are effective for non-invasive imaging of physiological properties, such as diffusion, vascularity and perfusion of the tissues of interest. However, the shortcoming of these agents limiting their broad application is its low sensitivity. The modification with targeting ligands, such as antibodies, proteins and peptides, even though improved probe delivery could not deliver a sufficient amount of agents to detect the target tissues<sup>2,3</sup>. Thereby nanoparticles have been used to load large amount of probes for increasing the local concentration of contrast agents<sup>2-4</sup>. The major limitation of nanoparticle-based MRI contrast agents is that they possess huge size when compared to the renal filtration threshold (~4.5 nm), and cannot be readily excreted from the body, resulting in toxic side effects. For example, systemic nephrogenic fibrosis, particularly in case of long-term tissue retention of high-dose Gd(III)-based MRI agents<sup>5-9</sup>.

The challenges in MRI for molecular imaging can be overcome by selection of molecular biomarkers and using MRI agents, which can readily be excreted from the body. Stable Gd(III) chelates, such as DOTA, DO3A, DTPA, have been proven safe and are receiving increasing attention as MRI agents<sup>2,7,10,11</sup>. For targeted contrast agents, the sufficiently expressed biomarkers at local position play a great role in molecular imaging. As previously reported, VEGF is strongly expressed in tumour tissues and its expression has been found to be proportional to the degree of malignancy for tumours<sup>12,13</sup>. VEGF binds the VEGFR2 receptor which is also strongly expressed in most tumour cells, as well as in endothelial cells that mediate tumour neovascularization<sup>14,15</sup>. Previously, VEGF<sub>125-136</sub>, a 12-amino acid peptide encoded by exon 6 of the VEGF gene, was found to block the specific binding of VEGF to the VEGFR2 receptor<sup>16</sup>. Based on these findings, it was hypothesized that targeted *in vivo* tumour imaging may be achieved with the use of

\*For correspondence. (e-mail: xyknfyf@126.com)



**Scheme 1.** Illustration of proposed VGd binding to tumour extracellular matrix for MR signal enhancement.

Gd(III)-based contrast agents labelled with the VEGF<sub>125-136</sub> peptide as depicted in Scheme 1. Furthermore, the use of VGd as a contrast agent would provide a more widely applicable agent based on the strong expression profile of VEGF in many tumours. Therefore, in the present study, VEGF<sub>125-136</sub> will be conjugated to Gd(III) through the formation of chelates and its ability to target VEGFR2 in BEL-7402 liver carcinoma cells both *in vitro* and *in vivo* will be investigated. Our study might develop a promising Gd(III)-based targeted MRI agent with high imaging efficacy for potential clinical use.

## Materials and methods

### Materials

All chemicals and solvents were used without further purification unless otherwise stated. The Fmoc-protected VEGF<sub>125-136</sub> peptide (QKRKRKKSRYKS) resin and its scrambled peptide (QKYSKQKKSSQKQK) resin were purchased from GL Biochem Ltd (China). 2-(1H-benzotriazol-1-yl)-1,1,3,3-tetramethyluronium hexafluorophosphate (HBTU), hydroxybenzotriazole (HOBt) and *N,N*-diisopropylethylamine (DIPEA) were from Aladdin. Gadoliniumacetic acid was from Strem Chemicals (USA). Piperidine was from Guangzhou Chemical Reagent Factory. DOTA-Tris (*t*-Bu ester) was from TCL (Tokyo, Japan).

### General method of characterization

Matrix-assisted laser desorption/ionization time-of-flight (MALDI-TOF) mass spectra were recorded on a Bruker Autoflex III MALDI-TOF MS in a linear mode. T1

relaxation constants were measured with a 3.0T MRI scanner (GE, Pittsburgh, USA) at 37°C in distilled water. The Gd concentration in VGd or SGd was determined with an inductively coupled plasma mass spectrometer (ICP-MS, Thermo Fisher, USA).

### Synthesis of Gd(III) chelates

The 12-amino acid VEGF<sub>125-136</sub> peptide (1.1 g) and the scrambled peptide (1.1 g) were deprotected with 15 ml piperidine/DMF solution (1 : 4, v/v) in solid phase peptide synthesis tubes to remove the Fmoc protecting groups. After washing with DMF (×3) and DCM (×3), DOTA-Tris (*t*-Bu ester) (290 mg, 0.5 mmol), HBTU (379 mg, 1 mmol), HOBt (100 mg) and DIPEA (500 μl) were added to each tube. The reaction continued under shaking at room temperature for 2 h. Then the resins were washed with DMF (×3) and DCM (×3) before cleavage with a mixture of trifluoroacetic acid/triisobutylsilane/water (96.5 : 1.0 : 2.5, v/v/v) for 5 h. The products were subsequently precipitated with cold diethyl ether twice and dried under reduced pressure at room temperature to yield VEGF<sub>125-136</sub>-DOTA or scramble-DOTA. MALDI-TOF (VEGF<sub>125-136</sub>-DOTA) (*m/z*, [M]<sup>+</sup>): 1978.36 (obsd.); 1978.15 (calcd). MALDI-TOF (scramble-DOTA) (*m/z*, [M]<sup>+</sup>): 2109.43 (obsd.); 2109.15 (calcd).

The dried sample was further dissolved in 3 ml double-distilled water, to which gadoliniumacetic acid (82 mg, 0.2 mmol) was added. During reaction, the pH was maintained at 6.5–7.0 at 50°C. After 24 h, the pH was adjusted to ~11 using aqueous NaOH (0.2 M) to remove most of the access Gd. Then the pH was neutralized to ~7 using HCl (0.2 M), followed by cold-drying to obtain crude

white products. Further, the products were purified using high-performance liquid chromatography (HPLC), with a C18 column used for the stationary phase and acetonitrile/water applied for the mobile phase. MALDI-TOF (VGd) ( $m/z$ ,  $[M]^+$ ): 2133.79 (obsd.); 2133.06 (calcd). MALDI-TOF (SGd) ( $m/z$ ,  $[M]^+$ ): 2264.05 (obsd.); 2264.35 (calcd).

### Cell culture

Human HCC cell line BEL-7402 (Chinese Academy of Medical Sciences, China) was grown in RPMI 1640 medium supplemented with 100 ml/l heat-inactivated fetal calf serum, 50,000 U/L penicillin and 50 mg/l streptomycin. The cells were cultured under a humid condition (95% relative humidity) at 37°C containing 5% CO<sub>2</sub>. The RPMI 1640 medium was refreshed every other day and the cells were split once the confluency was reached.

### In vitro MRI examination

BEL-7402 cells were grown in RPMI 1640 medium in cell culture flasks (25 cm<sup>3</sup>). When the cells reached 85% confluency, 100 µl of VGd (0.05 mmol/ml), 100 µl of SGd (0.05 mmol/ml) and 100 µl mixture of VGd and VEGF<sub>125-136</sub> as competitive probe test group (CPT, 0.05 mmol/ml, each) were added to flasks respectively. Thereafter, the cells were incubated for 24 h at 37°C under a humid condition at 5% CO<sub>2</sub>. After the cells were washed with PBS (×4) and trypsinized, the cells were transferred to centrifuge tubes, followed by addition of 0.6% agarose to form a suspension. A 3.0-T MRI scanner head coil was used to obtain an MRI scan of each tube with the following T1 scanning parameters: repetition time (TR)/echo time (TE) = 600/15 ms, matrix = 256 × 256, thickness = 2 mm, field of view (FOV) = 20 cm, (signal-to-noise ratio (SNR) = T1 mean signal/ambient noise) and region of interest (ROI) = 2 mm. ROI was selected as the diameter for an effective T1 measuring range.

### In vivo MR tumour imaging

Subaxillary xenografts of human BEL-7402 cells were established in 16 male nude mice (25–30 g, Slac Laboratory Animals Ltd, Shanghai, China). This animal study was approved by the independent ethics committee of Hainan Medical College Hospital, and all the animals received humane care throughout the duration of the study. When the tumour diameter reached ~1.0 cm, the mice were anesthetized with pentobarbital (0.05 mg/g, i.p.) and administrated with of VGd (100 µl, 0.2 mmol Gd/kg) and SGd (100 µl, 0.2 mmol Gd/kg) via tail vein injection. An additional 50 µl of saline was subsequently

administered to flush the line and ensure that the complete dose was administered in each mouse. The mice then went through an MRI examination with a 3.0-T MRI scanner (GE) that had a dedicated mouse MRI coil (Chenguang Medical Technologies Ltd, Shanghai). Seven scans were performed on each mouse: the first scan was performed prior to the administration of contrast administration (pre-injection), while the subsequent scans were performed at 5, 15, 30, 60, 120 and 240 min post-injection. All scans were conducted under the following axial fast-spin echo T1-weighted imaging conditions: TR/TE = 340/16 ms, number of excitations = 4, matrix = 128 × 128, FOV = 8 × 8 cm, slice thickness = 1.0 mm and slice interval = 0.1. Signal intensity was obtained by averaging three measurements for three ROIs within the same slice at various time points. The diameter of each ROI was ~2.0 mm.

### Immunohistological examination of VEGFR2 expression

For immunohistological staining of BEL-7402 xenografts, mice ( $n = 3$ ) were injected with VGd or SGd. Then, the tumours were fixed with 4% formaldehyde, dehydrated in a gradient alcohol series and xylene, and embedded in paraffin. Sections (5 µm) were cut from each tissue block and mounted onto slides. After the sections were incubated overnight at 60°C, the sections were immersed in xylene (5 min × 2) and then in a gradient alcohol series. After the sections were rinsed with water and 0.1 M PBS, they were immersed in methanol with 1% hydrogen peroxide at room temperature for 10 min before a final water rinse. The sections were subsequently treated with an antigen retrieval agent, rinsed with water, and blocked with non-immune horse serum. Subsequently, the sections were incubated with VEGFR2 antibody (Abcam) at 4°C overnight and then washed with 0.1 M PBS, followed by incubation with an appropriate biotinylated secondary antibody (Abcam) for 20 min at 37°C. After rinsing with PBS, the sections were then incubated with streptavidin-horseradish peroxidase at 37°C for 20 min. The bound antibodies were then visualized with 3,3'-diaminobenzidine. A final thorough washing of the sections was followed by a counterstaining step with hematoxylin.

### Biodistribution study

Tumour-bearing mice were sacrificed at 1 and 7 days post-injection. The tissues, for example, liver, lung, kidney, spleen, tumour, heart, brain, skin, femur and muscle were collected. After drying and weighing, each sample was fully immersed in 70% nitric acid (1.0 ml). Once the sample was completely liquefied, the solution was transferred to a new centrifuge tube (15 ml) and the

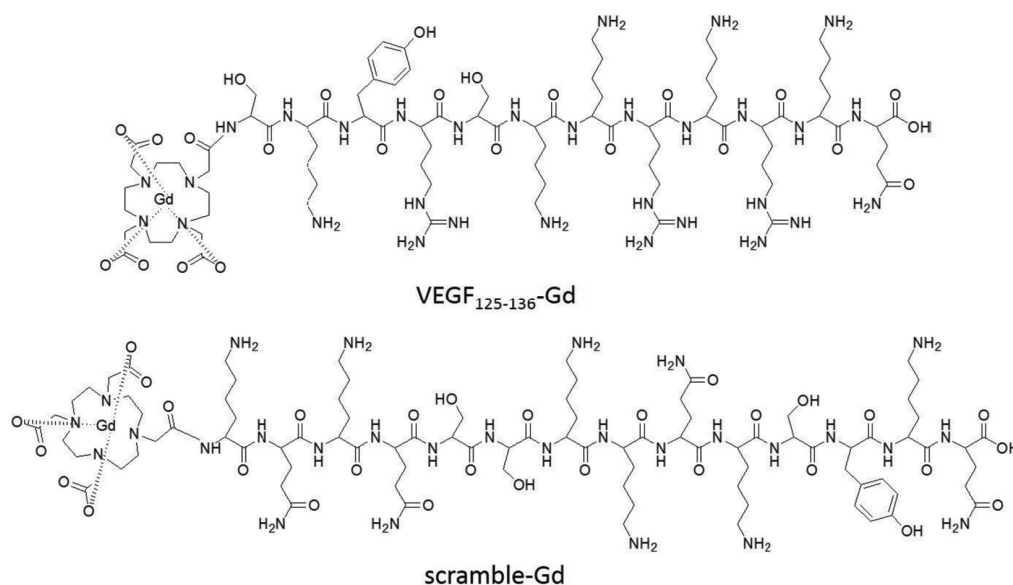


**Figure 1.** Chemical structures of VGd and SGd.

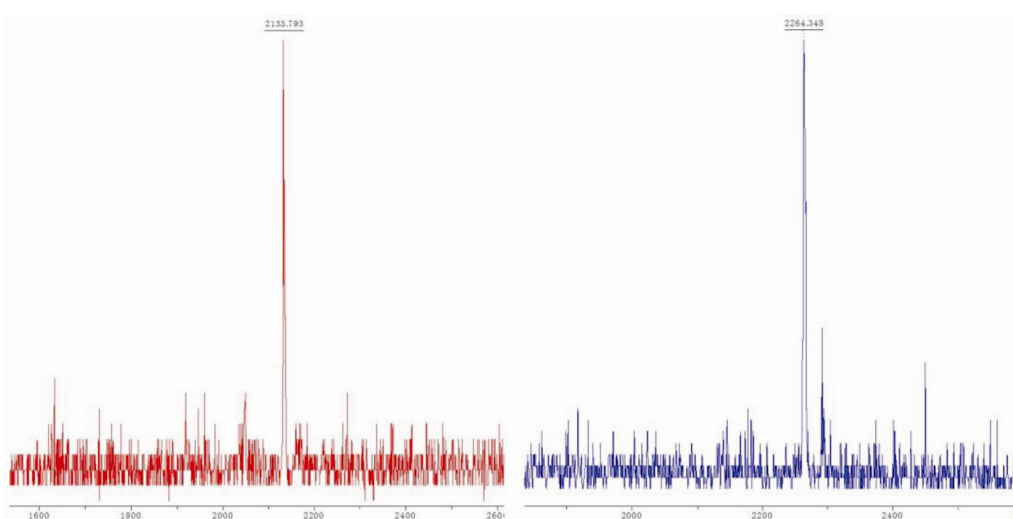


**Figure 2.** MALDI-TOF spectra of VGd and SGd.

undissolved components were spinned down at 10,000 rpm for 20 min. Then the solution was filtrated through a syringe filter (0.22  $\mu\text{m}$ , Nantong Feitebo Membrane Co Ltd, China) to further remove insoluble particles. Thereafter, the solution was diluted 10 times with deionized water and the Gd(III) concentration was detected by ICP. The average Gd(III) content in each tissue was calculated from the measured Gd(III) concentration and expressed as a percentage of injected dose per gram of organs (% ID/g).

## Results

The VGd and SGd in this study were purchased and used as received without further purification. After removal of

the Fmoc protecting group, the free amine groups directly conjugate with DOTA-Tris (t-Bu ester) through solid-phase chemistry as shown in Figure 1. Thereafter, the products were cleaved from resins and formed chelates with gadolinium through carboxyl groups. The chemical structures of VGd and SGd were confirmed with MALDI-TOF spectra as demonstrated in Figure 2, which was also described in the experimental section. The small peak that appeared to the right of the major peak in Figure 2 *b* should be ascribed to the addition of sodium element.

The plots of  $T_1$  and  $T_2$  water proton relaxation values at 3.0T versus the concentration of VGd or SGd are demonstrated in Figure 3. The  $T_1$  relaxivity values ( $r_1$ ) of VGd and SGd were measured to be  $7.15 \text{ mM}^{-1} \text{ s}^{-1}$  per Gd and  $7.46 \text{ mM}^{-1} \text{ s}^{-1}$  per Gd respectively. Also, their  $T_2$  relaxivity

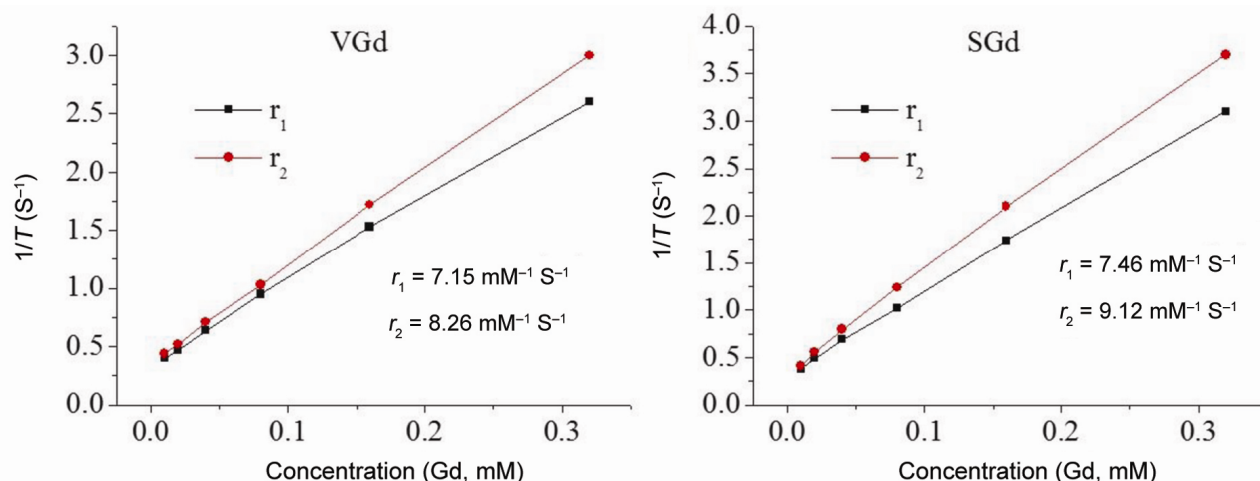


**Figure 3.** The plots of  $1/T_1$  and  $1/T_2$  versus the concentration of VGd and SGd.

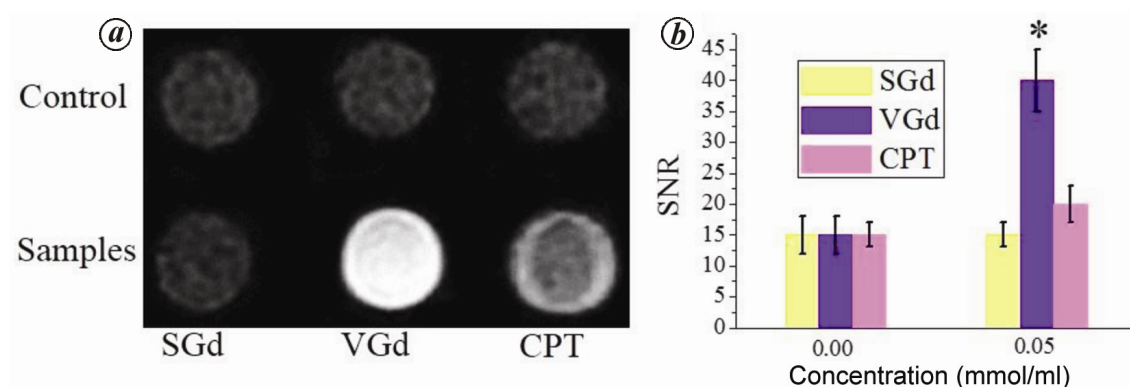


**Figure 4.** *a*, *In vitro* MRI scans of BEL-7402 cells treated and untreated with SGd, VGd and CPT respectively. *b*, The  $T_1$  signal-to-noise ratio values of the samples treated and untreated with SGd, VGd and CPT. \* $P < 0.01$  relative to others.

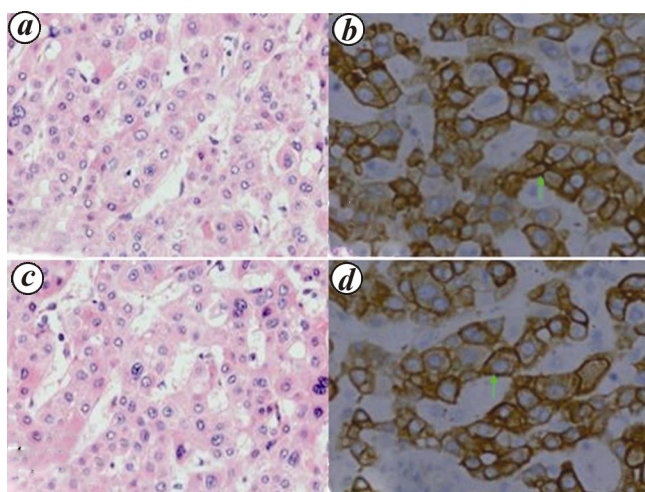


**Figure 5.** Immunohistochemical detection of VEGFR2 in tumour sections. Hematoxylin-eosin staining showing large nuclei (*a*) and cell membranes (*b*) positively stained for VEGFR2 for tumour sections used for treatment with VGd. Hematoxylin-eosin staining (*c*) and cell membranes (*d*) positively stained for VEGFR2 for tumour sections used for treatment with SGd. Green arrow indicates the VEGFR2 sites.

values ( $r_2$ ) were determined to be  $8.26 \text{ mM}^{-1} \text{ s}^{-1}$  per Gd and  $9.12 \text{ mM}^{-1} \text{ s}^{-1}$  per Gd respectively.

Figure 4 shows the results of the *in vitro* MRI examination of BEL-7402 cells treated with SGd, VGd and competitive group respectively. Clearly, the samples, untreated with agents, showed extremely poor contrast. A similar result was also observed for the sample treated with SGd. Conversely, the sample treated with VGd presented significant contrast enhancement. In addition, even though the sample treated with CPT showed slightly improved contrast than untreated groups, it was not comparable to the VGd-treated sample. Moreover, the  $T_1$  SNR was measured accordingly at the concentrations of 0.00 and 0.05 mmol/ml as shown in Figure 4*b*. Consistently, the VGd presented significantly higher SNR value than SGd and CPT groups.

To verify the targeting ability of VGd to VEGFR2 *in vivo*, it is paramount to confirm the availability of VEGFR2 in tumours. As shown in Figure 5, hematoxylin-eosin staining showed large nuclei with obvious isomerisms and visible mitotic figures and BEL-7402 tumour

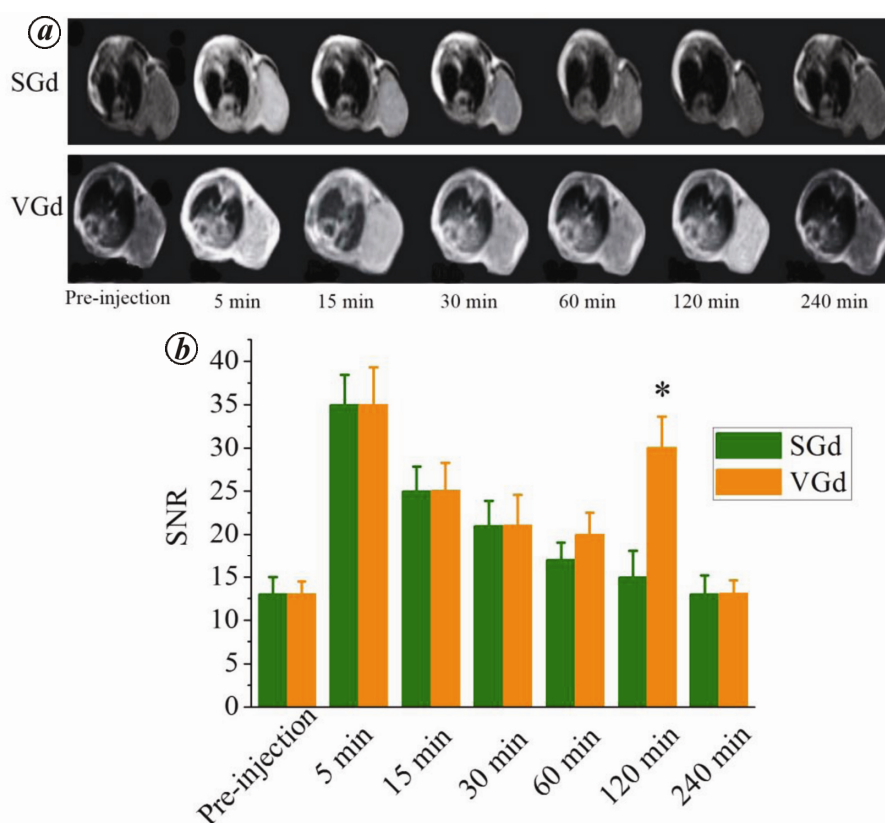


**Figure 6.** *a*,  $T_1$ -weighted MRI scans of tumour-bearing mice after tail vein injections of SGd or VGd. *b*, Comparison of  $T_1$  SNRs at various time points after the tail vein injections of SGd and VGd. \* $P < 0.01$  relative to SGd.

cell membranes positively displayed VEGFR2 for all tumour sections in the established xenografts of BEL-7402 cells. Hence, the tumours for VGd and SGd treatment in this study possessed the identical immunohistochemical conditions.

Further, the MRI scanning of tumour-bearing mice was performed to study the imaging effects of SGd and VGd as shown in Figure 6. The scanning time points were set at 5, 15, 30, 60, 120 and 240 min respectively. Apparently, the images recorded from both agents reached the brightest point at 5 min and showed contrast decrease with time. However, compared with SGd, the VGd group presented relatively higher contrast enhancement at the same time point after 5 min and, moreover, it showed much slower contrast decrease. Interestingly, it showed great contrast enhancement at 120 min. Subsequently, the SNR values corresponding to the images were measured and plotted as depicted in Figure 6b, showing the consistent results.

To evaluate the retention of contrast agents in the major organs, the biodistribution study was carried out at day 1 and day 7 post-injection in the tumour-bearing mice. The major organs were dissolved in high purity nitric acid and the Gd(III) content was measured by ICP. Figure 7 shows the biodistribution of SGd or VGd in the major organs, including muscle, femur, tumour, skin,

spleen, liver, kidney, lung, heart and brain at day 1 and day 7 post-injection at a dose of 0.2 mmol-Gd/kg. The retention of SGd and VGd was comparable in the normal tissues and was significantly different ( $P < 0.01$ ) in the tumour at day 1 post-injection. At day 7, the retention of VGd in tumour was still significantly higher than SGd ( $P < 0.05$ ).

## Discussion

Development of targeted MRI molecular probes is of great importance in molecular imaging since it has the potential to improve tumour visualization and positioning accuracy. Generally, the imaging component of probes includes iron- or Gd-based contrast agents, while the targeting ligands popularly studied are antibodies, peptides and aptamers. Peptides are particularly advantageous because of their low molecular weight, ease of transportation and storage, great stability and ease of modification<sup>17,18</sup>. For example, recent studies have demonstrated that the use of  $\alpha_v\beta_3$  integrin, aminopeptidase *N*, and angiopoietin could provide targeting of a tumour and its vascular endothelial cells<sup>19,20</sup>.

VEGF has 7 exon sequences and the affinity of peptide fragments encoded by these exons for VEGFR2 varies considerably. Previous findings suggested that the

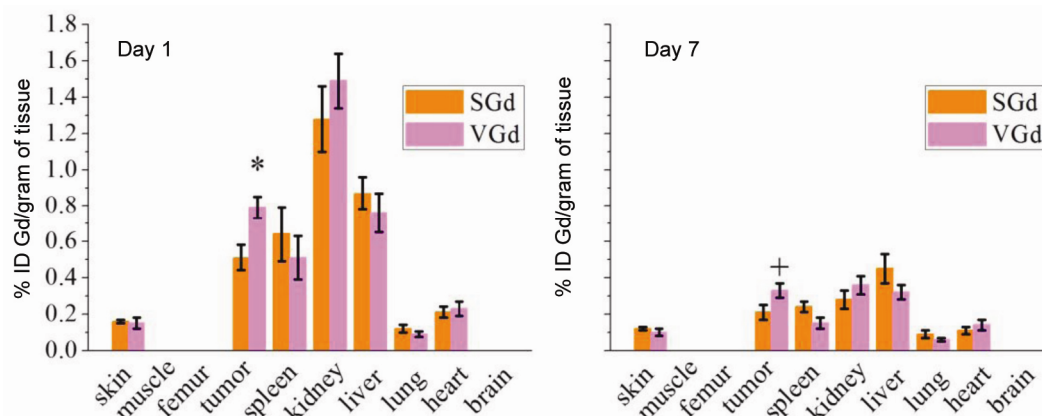


**Figure 7.** Biodistribution of gadolinium in the major organs and tissues of mice at day 1 and day 7 after administration of SGd and VGd at a dose of 0.2 mmol-Gd/kg in mice ( $n = 5$ ) bearing tumours. \* $P < 0.01$  and  $^+P < 0.05$  relative to SGd.

affinity of VEGF<sub>125-136</sub> (QKRKRKKSRYKS), a 12-amino acid peptide encoded by exon 6 for VEGFR2, was greater than that of other similar peptide fragments<sup>16</sup>. Furthermore, binding of VEGF<sub>125-136</sub> to the extracellular region of VEGFR2 has no biological activity, yet this binding event can competitively prevent the ability of VEGF from promoting tumour cell growth and angiogenesis. Therefore, irreversibly linking VEGF<sub>125-136</sub> with Gd via chemical bonds was expected to provide a targeted MRI imaging enhancement.

In the present study, we first synthesized VGd and SGd through a facile standard solid-phase chemistry as demonstrated in Figure 1. MALDI-TOF (Figure 2) was employed to confirm the molecular weights of VGd and SGd (2133.52 and 2264.60 g/mol respectively), and these weights matched their theoretical molecular weights, meaning that the chemical structures shown in Figure 1 were obtained. Furthermore, the relaxivity values including  $r_1$  and  $r_2$  at 3.0T for both SGd and VGd were confirmed as shown in Figure 3. The results indicated that both  $r_1$  and  $r_2$  of SGd were slightly higher than those of VGd. Earlier study on the MRI contrasts using CREKA as targeting peptide demonstrated that its  $r_1$  and  $r_2$  values were also slightly lower than those of the scrambled peptide<sup>11</sup>. However, the essential point in this study is to demonstrate the advantageous targeting ability of VGd over SGd. Therefore, the targeting effect will be valued more than the relaxivity, not to mention the slight difference between VGd and SGd. This question was further elucidated in the *in vitro* imaging study as indicated in Figure 4. In principle, the SGd with higher  $r_1$  value was expected to show enhanced contrast compared with VGd since MRI agents with higher relaxivity would provide equivalent contrast at a lower dose compared with lower relaxivity agents<sup>7,11</sup>. However, the results suggested that VGd with slightly lower  $r_1$  gave significantly greater imaging enhancement than SGd at the concentration of 0.05 mmol/ml than SGd, indicating that the targeting effect from VEGF<sub>125-136</sub> dominated the interaction of

agents with cells. To further confirm the targeting efficacy of VGd to cells, the competitive group was added and the cells showed much poorer imaging contrast than VGd, which might attribute to the competitive binding of VEGF<sub>125-136</sub> to VEGFR2. These imaging studies and the quantified SNR values in Figure 4b consistently demonstrated the great targeting efficacy of VGd to tumour cells.

To ensure the existence of VEGFR2 in tumours for both VGd and SGd groups, positive immune-histochemical staining of BEL-7402 cell membranes for VEGFR2 was employed for confirmation as shown in Figure 5, indicating the same tumour condition for both VGd and SGd groups. Further, tail vein injections of VGd or SGd were conducted to evaluate the *in vivo* imaging of contrast agents. It is found that efficient accumulation of the targeted contrast agent was observed in the tumour area at 5 min, however the contrast continuously decreased faster after 5 min for SGd than VGd. Previously, the other peptides used for MRI targeting imaging, including CREKA, ZD2 and CLT1, also indicated similar findings that agents modified with targeting peptides would provide enhanced contrast and also slower contrast decrease with scanning time<sup>2,11,21</sup>. As illustrated in Scheme 1, the VGd, once injected via tail vein, circulated in the blood vessel and conveniently bound to the VEGFR2 highly expressed in tumours, resulting in the improved tumour uptake of VGd compared with SGd. On the contrary, SGd without targeting function can be easily eliminated from the mouse body within short time post-injection, certainly strongly lowering its imaging efficacy. In addition, we noted that the contrast was sharply enhanced at 120 min for VGd. Previously, Gd-labelled VEGF monoclonal antibodies was injected via a caudal intravenous injection into a mouse model of a hepatocellular carcinoma (HCC) hepatic transplantable tumour, the contrast agent was detected at 10 min post-injection<sup>22</sup>. More interestingly, the highest contrast enhancement was detected at 120 min and the signal then disappeared completely within

24 h. These results agree with the present study, except that the signal for the contrast reagent was maintained for a longer period than that in the present study. It is possible that the larger molecular weight of the monoclonal VEGF antibodies in that study underwent longer circulation time.

The retention of both agents was comparable in the normal tissues and the VGd accumulation was significantly higher in the tumour post-injection as shown in Figure 7. The targeted contrast agent displayed higher tumour uptake than the non-targeted contrast agent. The injected agents were, mostly, eliminated from the mouse within short period. The kidneys and liver, the major organ involved in the excretion of contrast agents, had a Gd(III) retention of the injected VGd or SGd per gram of tissue, higher than other organs and tissues<sup>11</sup>. At day 7, the Gd(III) retention was remarkably decreased in the kidneys and liver. No detectable Gd(III) was observed in the bone, muscle or brain for SGd or VGd, indicating that our contrast agent should have great safety for potential clinical use. As compared with previously reported dendrimer-based targeted Gd(III) chelates, the peptide-targeted low molecular weight contrast agent, VGd, has much lower Gd(III) retention *in vivo*.

**Conflict of interest:** The authors declare no conflict of interest.

- Li, C. *et al.*, Gold-coated Fe<sub>3</sub>O<sub>4</sub> nanoroses with five unique functions for cancer cell targeting, imaging and therapy. *Adv. Funct. Mater.*, 2014, **24**, 1772–1780.
- Tan, M., Ye, Z., Lindner, D., Brady-Kalnay, S. M. and Lu, Z. R., Synthesis and evaluation of a targeted nanoglobular dual-modal imaging agent for MR imaging and image-guided surgery of prostate cancer. *Pharm. Res.*, 2014, **31**, 1469–1476.
- Li, J. *et al.*, A choline derivate-modified nanoprobe for glioma diagnosis using MRI. *Sci. Rep.*, 2013, **3**, 1623.
- Kuo, T. *et al.*, AS1411 aptamer-conjugated Gd<sub>2</sub>O<sub>3</sub>:Eu nanoparticles for target-specific computed tomography/magnetic resonance/fluorescence molecular imaging. *Nano Res.*, 2014, **7**, 658–669.
- Curtet, C., Maton, F., Havet, T., Slinkin, M., Mishra, A., Chatal, J. F. and Muller, R. N., Polylysine-Gd-DTPAn and polylysine-Gd-DOTAn coupled to anti-CEA F(ab')<sub>2</sub> fragments as potential immunocontrast agents. Relaxometry, biodistribution, and magnetic resonance imaging in nude mice grafted with human colorectal carcinoma. *Invest. Radiol.*, 1998, **33**, 752–761.
- Ke, T., Jeong, E. K., Wang, X., Feng, Y., Parker, D. L. and Lu, Z. R., RGD targeted poly(L-glutamic acid)-cystamine-(Gd-DO3A) conjugate for detecting angiogenesis biomarker alpha(v) beta 3 integrin with MRT, mapping. *Int. J. Nanomed.*, 2007, **2**, 191–199.
- Flacke, S. *et al.*, Novel MRI contrast agent for molecular imaging of fibrin implications for detecting vulnerable plaques. *Circulation*, 2001, **104**, 1280–1285.
- Amirbekian, V. *et al.*, Detecting and assessing macrophages *in vivo* to evaluate atherosclerosis noninvasively using molecular MRI. *Proc. Natl. Acad. Sci. USA*, 2007, **104**, 961–966.
- Sieber, M. A., Pietsch, H., Walter, J., Haider, W., Frenzel, T. and Weinmann, H. J., A preclinical study to investigate the development of nephrogenic systemic fibrosis: a possible role for gadolinium-based contrast media. *Invest. Radiol.*, 2008, **43**, 65–75.
- Tan, M. and Lu, Z. R., Integrin targeted MR imaging. *Theranostics*, 2011, **1**, 83–101.
- Zhou, Z., Wu, X., Kresak, A., Griswold, M. and Lu, Z.-R., Peptide targeted tripod macrocyclic Gd(III) chelates for cancer molecular MRI. *Biomaterials*, 2013, **34**, 7683–7693.
- Wang, Y. *et al.*, Bioinformatics analyses of the role of vascular endothelial growth factor in patients with non-small cell lung cancer. *PLoS One*, 2015, **10**, e0139285.
- Wang, S. W. *et al.*, CCL5/CCR5 axis induces vascular endothelial growth factor-mediated tumour angiogenesis in human osteosarcoma microenvironment. *Carcinogenesis*, 2015, **36**, 104–114.
- Pfister, N. T. *et al.*, Mutant p53 cooperates with the SWI/SNF chromatin remodeling complex to regulate VEGFR2 in breast cancer cells. *Genes Dev.*, 2015, **29**, 1298–1315.
- Smith, B. D. *et al.*, Altiratinib inhibits tumor growth, invasion, angiogenesis, and microenvironment-mediated drug resistance via balanced inhibition of MET, TIE2, and VEGFR2. *Mol. Cancer Ther.*, 2015, **14**, 1–12.
- Bainbridge, J. W. B., Jia, H., Bagherzadeh, A., Selwood, D., Ali, R. R. and Zachary, I., A peptide encoded by exon 6 of VEGF (EG3306) inhibits VEGF-induced angiogenesis *in vitro* and ischaemic retinal neovascularisation *in vivo*. *Biochem. Biophys. Res. Commun.*, 2003, **302**, 793–799.
- Naganna, N. and Madhavan, N., Soluble non-cross-linked poly(norbornene) supports for peptide synthesis with minimal reagents. *J. Org. Chem.*, 2014, **79**, 11549–11557.
- Baxter, D., Ullman, C. G. and Mason, J. M., Library construction, selection and modification strategies to generate therapeutic peptide-based modulators of protein-protein interactions. *Future Med. Chem.*, 2014, **6**, 2073–2092.
- Yang, Y., Zhou, J. and Yu, K., Design, synthesis, and *in vitro* evaluation of a binary targeting MRI contrast agent for imaging tumour cells. *Amino Acids*, 2014, **46**, 449–457.
- Debergh, I. *et al.*, Molecular imaging of tumor-associated angiogenesis using a novel magnetic resonance imaging contrast agent targeting  $\alpha_v\beta_3$  integrin. *Ann. Surg. Oncol.*, 2014, **21**, 1–8.
- Han, Z. *et al.*, EDB Fibronectin specific peptide for prostate cancer targeting. *Bioconjug. Chem.*, 2015, **26**, 830–838.
- Leung, K., Antivascular endothelial growth factor poly(lactic acid)-poly(ethylene glycol)-poly-L-Lys/gadolinium-diethylenetriamine pentaacetic acid nanoparticles. Molecular Imaging and Contrast Agent Database (MICAD) (internet). Bethesda (MD): National Center for Biotechnology Information (US); 2004–2013. 5 May 2012 (updated 19 July 2012) (PubMed: 22812022).

**ACKNOWLEDGEMENTS.** We thank Zheng-Rong Lu (Department of Biomedical Engineering, Case Western Reserve University, Cleveland, OH) for his guidance in the probe construction efforts. This study was funded by the National Natural Science Foundation of China (Grant nos 81160177, 81641067 and 81460262) and the Natural Science Foundation of Hainan, China (Grant no. 20158290).

Received 14 September 2016; revised accepted 11 April 2017

doi: 10.18520/cs/v113/i05/869-876